N O T I C E

THIS DOCUMENT HAS BEEN REPRODUCED FROM MICROFICHE. ALTHOUGH IT IS RECOGNIZED THAT CERTAIN PORTIONS ARE ILLEGIBLE, IT IS BEING RELEASED IN THE INTEREST OF MAKING AVAILABLE AS MUCH INFORMATION AS POSSIBLE

NASA TECHNICAL MEMORANDUM NASA TM-75763

EXPERIMENTAL ANALYSIS OF THE BOUNDARY LAYER TRANSITION WITH ZERO AND POSITIVE PRESSURE GRADIENT

Arnal, D., Jullen, J.C., and Michel, R.

Translation of "Analyse expérimentale de la transition de la couche limite avec gradient de pression nul ou positif", Office National D'Etudes Et De Recherches Aérospatiales, Chatillon (France), Report TP no. 1979, 14 p. (21st Annual Conference on Aviation and Astronautics, Tel Aviv and Haifa, Israel, Feb. 28-Mar. 1, 1979)

NATIONAL AERONAUTICS AND SPACE ADMINISTRATION
WASHINGTON, D.C. 20546 FEBRUARY 1980

STANDARD TITLE PAGE

1. Report No.	2. Government Accession No.	3. Recipient's Catalog No.
NASA TM-75763		

4. Title and Subtitle	5. Report Date
EXPERIMENTAL ANALYSIS OF THE BOUNDARY LAYER TRANSITION WITH ZERO AND POSITIVE PRESSURE GRADIENT	February 1980
	6. Performing Organization Code

7. Author(s)	8. Performing Organization Report No.
Arnal, D., Jullen, J.C., and Michel, R. Office National d'Etudes et de Recherches Aérospatiales, Chatillon, France)	10. Work Unit No.
	11. Contract or Grant No. NASW-3199
9. Performing Organization Name and Address: Leo Kanner Associates, Recwood City, Ca. 94063	13. Type of Report and Period Covered: Translation
12. Sponsoring Agency Name and Address: National Aeronautics and Space Administration, Washington, D.C. 20546	14. Sponsoring Agency Code

15. Supplementary Notes

Translation of "Analyse expérimentale de la transition de la couche limite avec gradient de pression nul ou positif", ONERA, TP no. 1979-8, 14p. (Annual Conference on Aviation and Astronautics, 21st, Tel Aviv and Haifa, Israel, Feb28-Mar 1, 1979), pp 1-13 (A79-50922)

16. Abstract

This study is concerned with the influence of a positive pressure gradient on the boundary layer transition. Four cases are experimentally studied by measuring the mean velocity and turbulence profiles. As the intensity of the pressure gradient is increased, the Reynolds number of the transition onset and the length of the transition region are reduced. By a more detailed study, we can observe the Tollmien-Schlichting waves disturbing the laminar regime; the amplification of these waves is in good agreement with the stability theory. The three-dimensional deformation of the waves leads finally to the appearance of turbulence. In the case of zero pressure gradient, the properties of the turbulent spots are studied by conditional sampling of the hot-wire signal; in the case of positive pressure gradient, the turbulence appears in a progressive manner and the turbulent spots are much more difficult to characterize.

17. Key Words (Selected by Author(s))	18. Distribution Statement
	Unclassified-Unlimited

19. Security Classif. (of this report)	20. Security Classif. (of this page)	21. No. of Pages	22. Price
Unclassified	Unclassified	30	

NASA-HQ

ANNOTATIONS

x : Abscissa measured on the axis beginning with the stop-point.

y : Ordinate counted from the wall.

t : Time.

U : Mean longitudinal velocity ; U_e external velocity at the boundary layer.

u' : Longitudinal fluctuation

$\overline{u'^2}$: Quadratic mean of u'

U_{ref} : Reference velocity

α : Half angle of the pipe divergence

δ : Physical thickness of the boundary layer

δ_1 : Displacement density $\delta_1 = \int_0^\delta (1 - \frac{U}{U_e}) dy$.

θ : Momentum density $\theta = \int_0^\delta \frac{U}{U_e}(1 - \frac{U}{U_e}) dy$

H : Boundary layer shape parameter

R_x, R_θ : Reynolds numbers

f : Frequency

$\overline{e'^2}$: Turbulent energy per Hz such that $\int \overline{e'^2}\, df = \overline{u'^2}$

INDEXES

e : Outside of the boundary layer

T : Transition onset

f : Transition completion

l : Laminar

P : Point

t : Turbulent

EXPERIMENTAL ANALYSIS OF THE BOUNDARY LAYER TRANSITION WITH ZERO AND POSITIVE PRESSURE GRADIENT

Daniel Arnal, Jean-Claude Juillen, Roger Michel
ONERA; Centre d'Etudes et de Recherches de Toulouse (CERT)

SUMMARY

This study is concerned with the influence of a positive pressure gradient on the boundary layer transition. Four cases are experimentally studied by measuring the mean velocity and turbulence profiles. As the intensity of the pressure gradient is increased, the Reynolds number of the transition onset and the length of the transition region are reduced. By a more detailed study, we can observe the Tollmien-Schlichting waves disturbing the laminar regime; the amplification of these waves is in good agreement with the stability theory. The three-dimensional deformation of the waves leads finally to the appearance of turbulence. In the case of zero pressure gradient, the properties of the turbulent spots are studied by conditional sampling of the hot-wire signal; in the case of positive pressure gradient, the turbulence appears in a progressive manner and the turbulent spots are much more difficult to characterize.

/1*

1 - INTRODUCTION

It has been known for a long time that the longitudinal pressure gradient is one of the main factors affecting the onset of the transition of a laminar boundary layer; its effect has been taken into account in a certain number of empirical criteria, such as those of Michel (1) or of Dunham (2). Unfortunately, in most cases, experiments serving as a basisfor establishing these criteria are not sufficiently detailed and provide only partial information on the processes of the appearance and development of turbulence.

The objective of this report is not to confirm or to attack the validity of existing empirical criteria, but to present thorough

*Numbers in the margin indicate pagination in the foreign text.

experimental results of the mean and fluctuating quantities measured in the laminar regime and in the transition zone. Only natural transition cases are considered here, and the artifices sometimes used for the study of certain special effects are excluded: (vibrating ribbon, controlled three-dimensionality, electrical discharges which create turbulent spots). Moreover, in all of the cases examined, the transition occurs prior to the laminar separation.

First, we have attempted to obtain an over-all description of the effects of traditional measurements (mean values resulting from an integration over a long period of time); such measurements prove to be inadequate for determining the basic mechanisms. A second phase of the study was conducted to bring these mechanisms to light and to investigate them qualitatively by a conditional analysis of the hot-wire signal; this type of analysis made it possible to evaluate the effect of the pressure gradient on the processes of establishing the turbulent boundary layer.

2 - EXPERIMENTAL SET-UP AND MEANS OF MEASUREMENT - TEST CONDITIONS

2.1. Experimental Set-Up and Means of Measurement

The boundary layer transition is studied on a cylindrical body, 6 cm in diameter placed behind an ogive-shaped body along the axis of a revolving pipe, the conicity of which determines the pressure distribution in the potential flow. The total length of the main body is 1.20 m. The wind tunnel, which operates by the suction of ambient air, is described in detail in (3).

The measurements are performed with constant temperature hot-wire anemometers. A slow collection chain (10 points per second) makes it possible to obtain profiles of average velocity and turbulent quantities, along with parameters which are characteristic of the boundary layer.

We have conducted a more thorough investigation of the fluctuation of u' by processing on a computer the hot-wire signal digitized

for 6 seconds at the rate of 10,000 points per second. We have thus been able to calculate the moments of order 3 and 4 of the fluctuation and to obtain numerical spectra by means of a program of the rapid Fourier transformation curve, with the analysis band being 10 Hz. Finally, the study of certain special effects (intermittence, "points"), has called for a conditional analysis of the instantaneous velocity. Additional information on the collection chain and on the conditional sampling technique may be found in (4) and (5).

2.2. - Test Conditions

Four configurations have been studied. The distributions of the corresponding external velocity are plotted on figure 1; the values of $U_{ref.}$ (reference velocity measured at the connection of of the ogive-shaped body and the cylindrical body) and of α (semi-angle of the pipe divergence) are given in the table below:

Configuration	U_{ref} (m/s)	α (°)
A	33	0.2
B	28	0.7
C	17	0.7
D	21	0.9

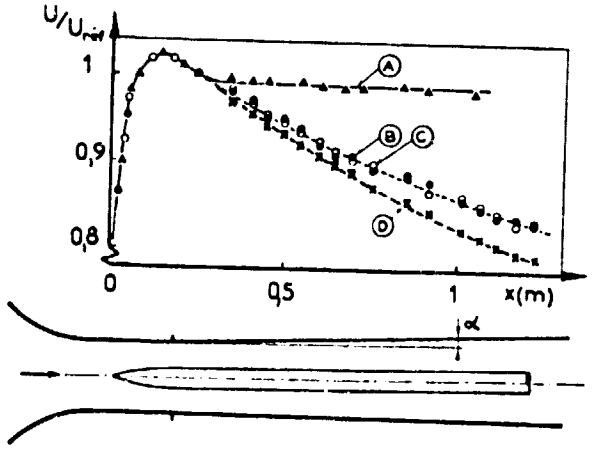

Fig. 1 - External Velocity Distribution

For x greater than 0.2 m, 0.2 m, the configuration A corresponds roughly to the case of the flat plate uniform flow, the moderate divergence at the pipe is intended to compensate for the thickening effect of the boundary layers. In fact, this divergence has been somewhat overestimated, so that a small deceleration of the flow toward the downstream may be observed. The configuration will nevertheless be called "flat plate configuration", since the parameter values of the shape H found in the laminar regime

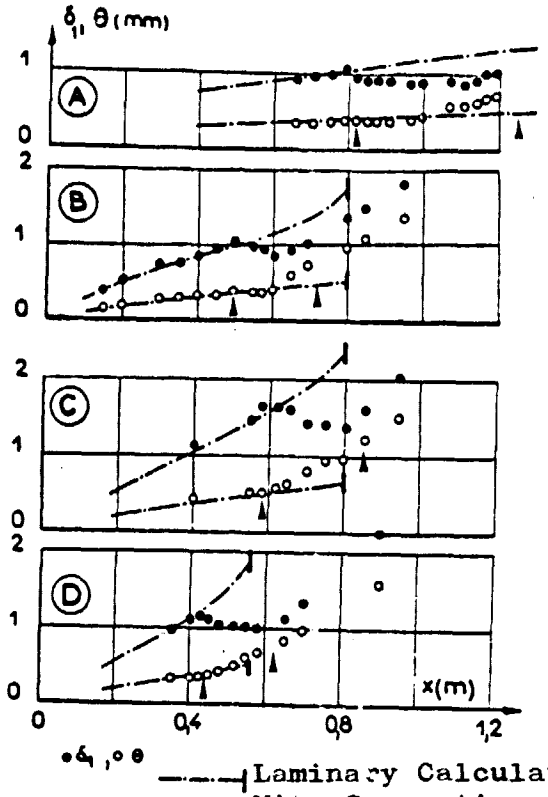

δ1, θ ——— Laminary Calculation
With Separation

Fig. 2 - Integral Density Variations

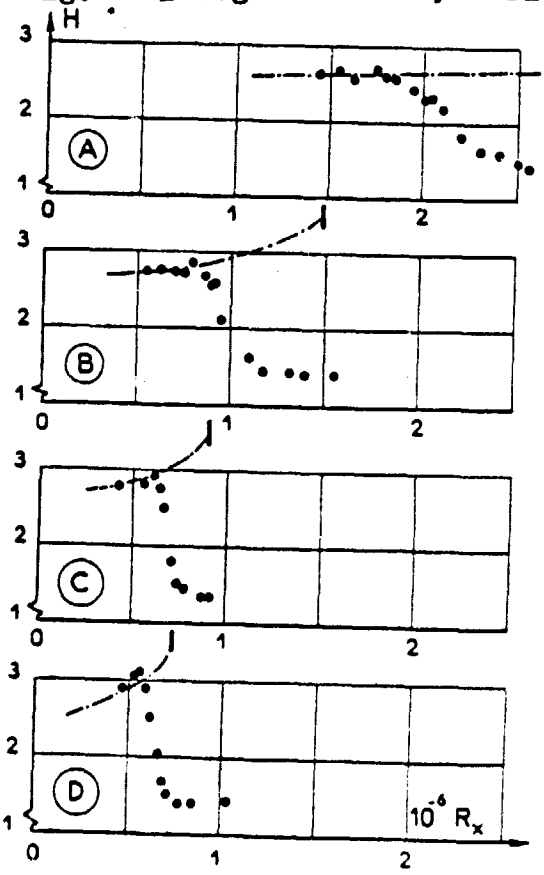

——— Laminary Calculation With Separation

Fig 3 - Shape Parameter

are extremely close to the theoretical value of the Blasius profile.

Configurations B, C and D correspond to the cases of clearly decelerated flows. The same pipe has been used to construct configurations B and C, which mainly differ by the value U_{ref}.

Besides the longitudinal pressure gradient, we are assuming that the only parameter affecting the Reynolds transition number is the turbulence of the general flow; we have found for the four cases values of the longitudinal turbulence rate $\sqrt{u^2}/U_e$, of about 0.2 %. The frequency range for the energy ranges between 0 and 200 Hz approximately.

3 - GENERAL STUDY OF THE TRANSITION

The expression "general study" means here the gross results provided by the anemometric chain by performing averages over theoretically infinite and practically very long times. The quantities studied are the mean velocity U and the turbulent energy $\overline{u^2}$.

3.1. - Average Velocity. Characteristic Parameters

The variation of the integral thicknesses δ_1 and θ as a function of the abscissa x is plotted on figure 2, for the four configurations studied; figure 3 shows the variation of the shape parameter H as a function of the Reynolds number R_x. A calculation of the laminar boundary layer by a technique of finite differences has been performed in each case: the theoretical variations of the quantities δ_1, θ and H are also shown on figures 2 and 3.

In a first analysis, we may consider that the transition onset appears when H begins to decrease, and it is completed when H is almost constant. Up until the beginning of the transition, the experimental measurement of the quantities under consideration is in good agreement with the theoretical curves. It should also be observed that the calculation gives for configurations B, C and D a laminar separation which is clearly located downstream at the transition onset.

Conf.	x_T (m)	x_f (m)	H_T	R_{θ_T}	R_{θ_f}
A	0.82	(1.27)	2.65	850	(1750)
B	0.50	0.75	2.85	690	1320
C	0.58	0.85	2.95	580	1250
D	0.44	0.64	3.05	540	950

The table to the left gives a certain number of characteristics relating to the four cases studied; the index T designates the point of transition onset where the decrease of H begins and the index f relates to the end of transition.

Let us make first two remarks concerning configuration A: on the one hand, the value H_T (2.65), moderately higher than the value 2.59 of the Blasius profile, is the indication of a very moderate positive pressure gradient; on the other hand, the values of x_f and $R_{\theta f}$, shown between parenthesis, are extrapolated values, because at the last probe station accessible on the experimental set-up (x = 1.19 m), the shape parameter does not seem to have reached a turbulent asymptotic value.

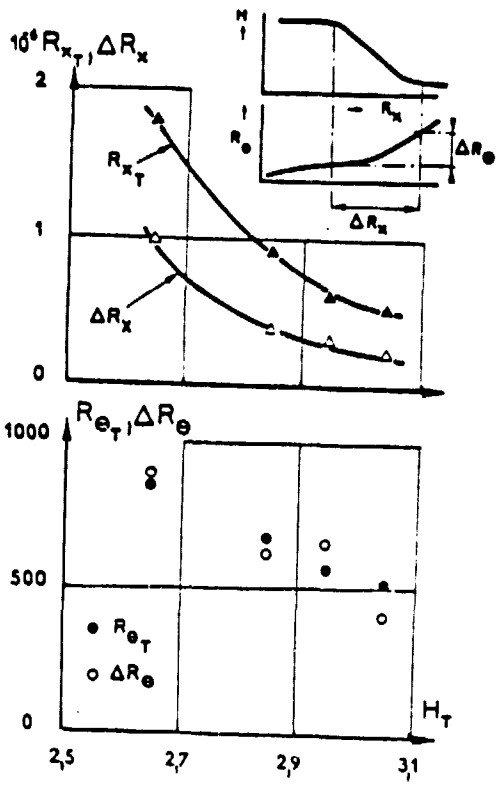

Fig. 4 - Reynolds Numbers at transition onset. Length of transition.

It is obvious that the choice of x_T and x_f (which in fact determines H_T, $T_{\theta T}$ and $R_{\theta f}$) is rather subjective; nevertheless, beyond the experimental error range, there is a distinct decrease in R_{XT} and $T_{\theta T}$ when H_T increases, hence the intensity of the pressure gradient (H_T may be considered as a pressure gradient parameter, since it is bound on a one-to-one basis to the dihedral angle β and to the parameter $\Lambda_2 = -\frac{\theta^2}{\nu}\frac{dU_e}{dx}$) for similar solutions).

The variations of R_{XT} and $R_{\theta f}$ as a function of H_T are plotted on figure 4 with those of $\Delta R_x = R_{xf} - R_{xT}$ and $\Delta R_\theta = R_{\theta f} - R_{\theta T}$. It may be seen that ΔR_x is also a decreasing function of H_T, i.e. that the length of the transition zone diminishes when the intensity of the pressure gradient increases. As for ΔR_θ, it varies closely with $R_{\theta T}$: this property may be used in a method where the calculation of the transition from the laminar to the turbulent flow is performed by using a weighted factor, which is a function of $R_\theta/R_{\theta T}$, beginning with zero for $R_\theta = R_{\theta T}$ and reaching the value 1 for $R_\theta \geq 2R_{\theta T}$.

On the left part of figure 5, experimental profiles of mean velocity at the end of the laminar regime are plotted for configurations A and D where the H_T (therefore the $R_{\theta T}$) differ the most; the distance to the wall is rendered dimensionless by density. We have also shown on this figure the theoretical profile of Blasius, which is not very different from the experimental profile of case A. On the other hand, the profile corresponding to configuration D makes a distinct inflexion point appear at $Y/\delta \simeq 0.6$; as we

will see later on, the theory of laminar instability shows a mean velocity profile which has a very unstable inflexion point. This instability results in a much faster transition for a profile without a point of inflexion.

If the experimental profiles $\frac{u}{u_e}(y/\delta_1)$ obtained at the end or after the end of transition (right section of figure 5) are now taken into consideration for various configurations, it may be stated that these profiles are practically intermingled: the shape parameters are very close to 1.4. It may thus be observed that the pressure gradients involved are important for the laminar regime, but insignificant for the "turbulent" regime at the end of transition.

3.2. - Profiles of Longitudinal Turbulence Intensity

The profiles of longitudinal turbulence $\sqrt{\overline{u^2}}/u_e$ are plotted on figures 6 and 7. In order to compare their variation from one case to another, we have presented for each configuration: two profiles in the first part of the transition, one in the middle of transition, two in the second part of transition and one in the "established" turbulent regime (except for case A where the turbulent regime does not appear to be completely reached at the last probe station). This delineation of study regions is certainly arbitrary, but it makes it possible to detect possible deformations in turbulence profiles when the pressure gradient varies.

At first sight, the general variation of the shape of the profiles is identical for the four configurations. At the transition onset, the profiles present a maximum level located toward the third part or the middle of the boundary layer thickness; this appearance occurs, moreover, for all of the profiles measured in the laminar regime, upstream from the transition point, with the maximum intensity increasing gradually with the abscissa up to values of 2 or 3 percent. When the transition begins (let us recall that the word "transition" here means "a decrease in the shape parameter"); it reaches its highest value, of about 20 percent

toward the middle of the transition and then decreases slowly until it reaches the turbulent regime.

A rather distinct difference exists, however, between configuration A and the configurations with the pressure gradient: toward the middle of the transition of the "flat plate" case, a local maximum appears on the profiles at an altitude of about 2 millimeters. This maximum, which remains in the second part of the transition, does not appear as exaggerated on the other configurations: the profiles simply present a more or less distinct flat part.

Let us now take into consideration the profiles measured near the abscissa at the end of transition X_f, with the occurence of $x = 1.19$ (case A), $x = 0.70$ m (case B), $x = 0.85$ m (case C), $x = 0.65$ m (case D); it appears immediately that these profiles are rounder and fuller (presence of second maximum level or of flat part previously mentioned) than the profiles measured downstream in the turbulent regime. The latter are quite similar to the "standard" profile of the standard turbulent (see Klebanoff (6)); the shape parameter nevertheless has not varied much from one station to the other. We see here how arbitrary the definition of an "end of transition" abscissa based only on the shape parameter can be.

To conclude, we can state that in spite of a few apparently minor differences, the four cases studied have a rather large similitude in the variation of the turbulence profiles. Moreover, it is obvious that the measurement of only global quantities (mean velocity and turbulence) is quite inadequate for the determination of the real effects of the transition process. We shall see in the following paragraph that these effects are in fact quite different from one case to another.

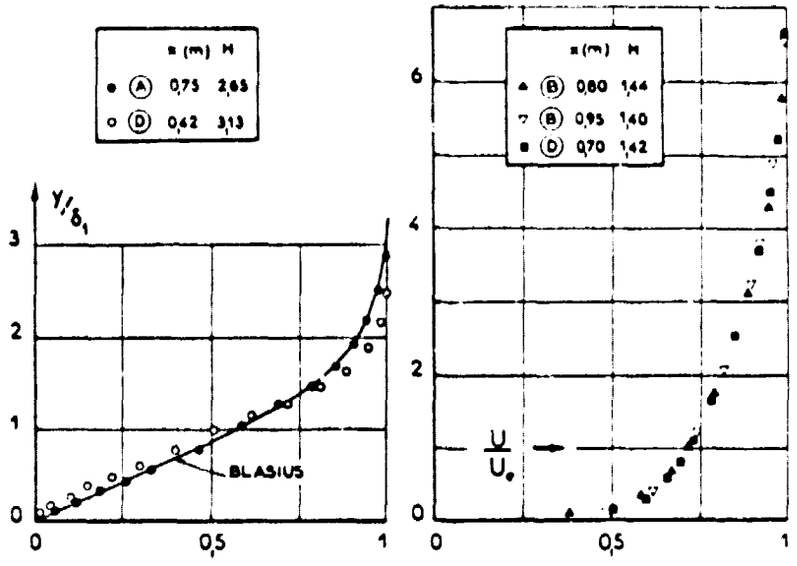

Fig. 5 - Examples of Transition Onset and Completion Mean Velocity Profiles

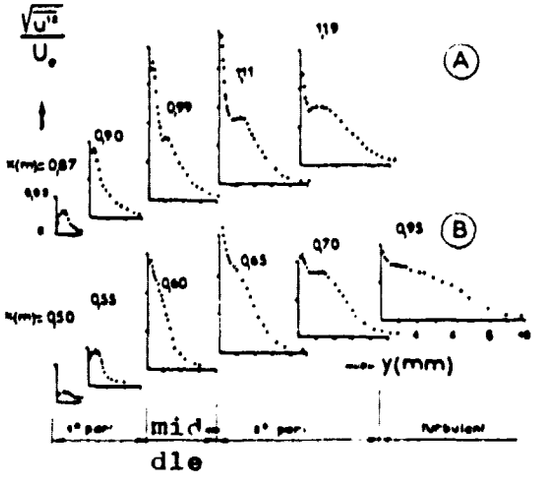

Fig. 6 - Turbulence Profiles (Configurations A & B)

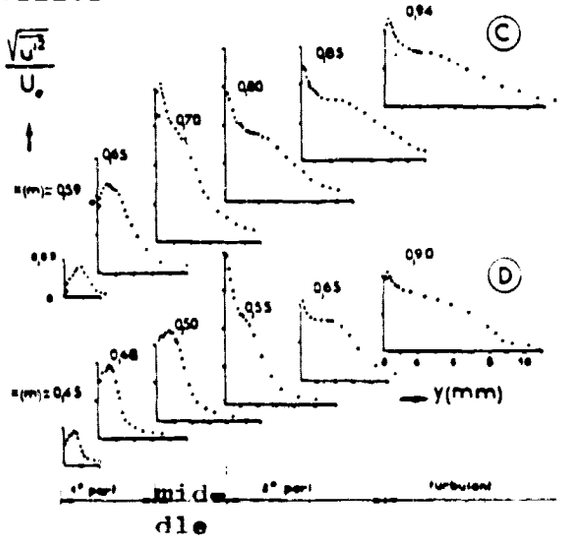

Fig. 7 - Turbulence Profiles (Configurations C & D)

4 - DETAILED STUDY OF THE TRANSITION PROCESS

The objective of this pragraph is to describe in detail the fundamental mechanisms of the transition onset and of the laminar state to the turbulent state, by attempting to bring to light the effect of the pressure gradient on these processes: this is why two extreme configurations shall be compared, i.e. configuration A - flat plate - and configuration D (value of H_T is the highest of the various cases studied). We shall refer to qualitative results (appearance of hot-wire signals) as well as to quantitative results (conditional analysis), and this is for typical abscissa selected successively in the laminar regime, at the transition onset, in the middle of transition and at the end of transition. 16

4.1. - Laminar State

4.1.1. - Qualitative Study

Figure 8 shows two examples of recordings which bring to light the instability causing the transition onset. These recordings, performed near the wall for two different abscissas, relate to configuration D; qualitatively, analogous effects appear in three other cases, but they are more clearly illustrated in this configuration.

In x = 0.35 m, the instantaneous velocity is the sum of low frequency fluctuations, with an irregular appearance, and of higher frequency fluctuations with a more regular appearance and a smaller amplitude. The spectrum makes it possible to determine the corresponding frequency ranges: from 0 to 100 Hz for low frequency fluctuations around 360 Hz for oscillations with sinusoidal appearance.

In x = 0.425 m, the signal u'(t) and the corresponding spectrum show a distinct evolution in the relative importance of the various frequencies: the amplitude of low frequencies is about the same as for the preceding station: on the other hand, the fluctuations with sinusoidal appearance, insignificant in x = 0.35 m, have become

predominant: the spectrum is reduced practically to a point centered around 360 Hz. These sinusoids (with modulation effect) correspond to the Tollmien-Schlichting waves, identified for the first time in the natural transition by Schubauer-Skramstad (7) and described by the theory of laminar instability.

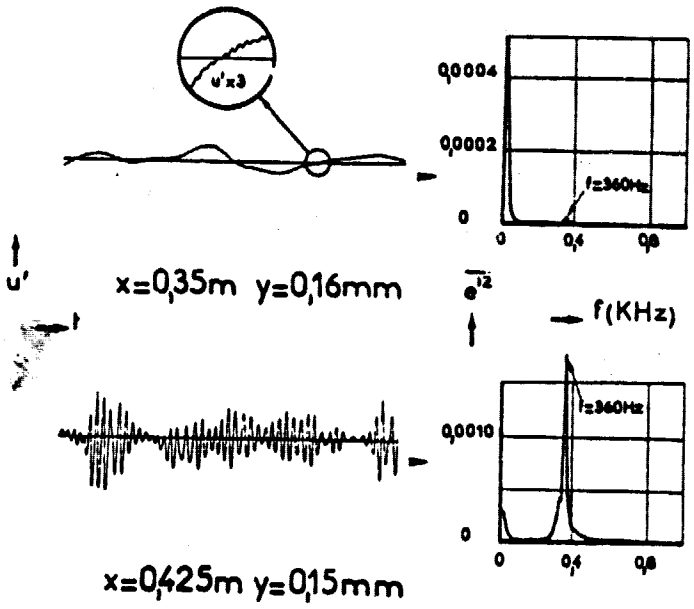

Figure 8 - Presentation of Tollmien-Schlichting waves (configuration D).

4.1.2. - Laminar Instability

It is not our intention to present in detail a theory which has amply appeared in publications since the first works of Tollmien and Schlichting (see, for example Schlichting (8), Jordinson (9), Mack (10) ...). We will concentrate on describing the principle and the results which apply to our experiments.

The principle of the theory of laminar instability is to introduce in the Navier-Stokes equations small perturbations with a certain mathematical shape and to calculate as a function of their frequency their wave length and the Reynolds number, whether they are likely to be amplified or dampened. We are assuming that u' has the following shape (spatial theory):

$$u' = f(y)\, e^{-\alpha_i x}\, e^{i(\alpha_r x - \omega t)}$$

u' is thus the product of an amplitude function f(y), of an amplitude term $(\alpha_i < 0)$ or of damping $(\alpha_i > 0)$ and a periodic term.

The resolution of stability equations requires the mean velocity profile to be introduced as given $\frac{U}{U_e}(Y/\delta)$. Its shape has a considerable effect on the digital results; for example, a profile presenting a point of inflexion $(dp/dx > 0)$ is much more unstable than a profile without point of inflexion $(dp/dx \leq 0)$: the range of frequencies likely to be amplified and the value of the amplification coefficients cross rapidly with the parameter of the shape H. 17

With respect to configurations A and D, we have shown below the theoretical values of the amplification coefficients obtained on the instability diagrams calculated by Landahl (11) for various base profiles. We have taken into consideration the frequency corresponding to the peak of spectra of u', for Reynolds numbers R_{δ_1} close to $R_{\delta_{1T}}$:

Configuration	f (Hz)	R_{δ_1}	$-\alpha_i$
A	600	2 000	$\simeq 5$
D	360	1 500	42.5

4.1.3. Comparison with the Experiment

A comparison between experimental and theoretical values for the amplification coefficient $-\alpha_i$ has been made in case D, for frequency 360 Hz. With this objective, we first of all measured the spectra of u' at various abscissa located upstream from the transition point, and this for an altitude of twelve at each abscissa.

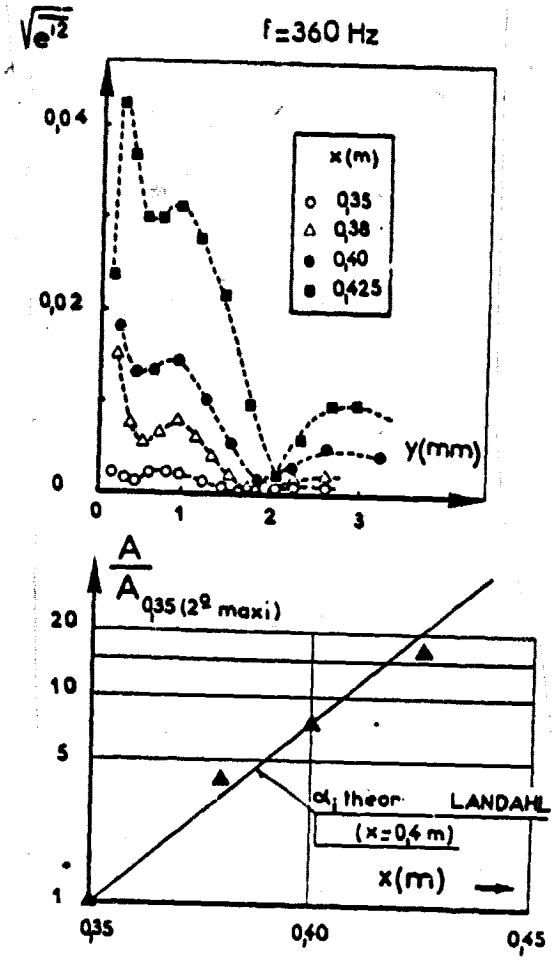

Fig. 9 - Amplification of the Tollmien-Schlichting waves (configuration D).

variation along x of the amplitude profiles for F = 360 Hz. These profiles, plotted on figure 9 present three maximum levels: the first near the wall, the second for y congruent to 0.9 mm, the third toward the outside of the boundary layer. We have shown to the left on figure 9 the variation along x of the quantity $\ln A/A_{0,35}$, where A stands for the amplitude of the second maximum level, with the index 0.35 relating to the first abscissa considered. The theoretical slope $-\alpha_i = d(\ln A)/dx$ is also plotted on this figure: a satisfactory agreement may be observed between the experimental amplification and that given by the theory.

In a previous report (3), we were able to observe that in the first centimeters prior to the transition onset, the frequency 600 Hz of configuration A coincided quite well with the theoretical laws. In fact, in the stability diagram for the Blasius profile, this frequency is located very near the upper section of the neutral curve and the experiment revealed that it was not very amplified.

4.2. - Transition Onset

The theory of laminar instability, which describes the development of the Tollmien-Schlichting waves, is a linearized theory; the purpose of this paragraph is to investigate the nonlinear effects which mark the end of the domain of theoretical application and which will lead rather quickly to the appearance of turbulence.

4.2.1 - Case of the Flat Plate

The only measurements with the hot-wire are obviously not sufficient for obtaining a real physical description of the processes leading to the creation of turbulence; visualization processes prove to be very useful, even indispensable, for the qualitative understanding of the occurances. To illustrate our measurements, we have chosen to refer to the Knapp-Roache-Mueller (12) smoke visualizations. The main reason for this is that these authors work with a set-up similar to ours : a cylindrical body placed behind an ogive-shaped body longitudinally in the direction of the flow.

Figure 10 shows a synthesis of the visualizations performed by Knapp et al, together with examples of hot-wire signals obtained in our experiments.

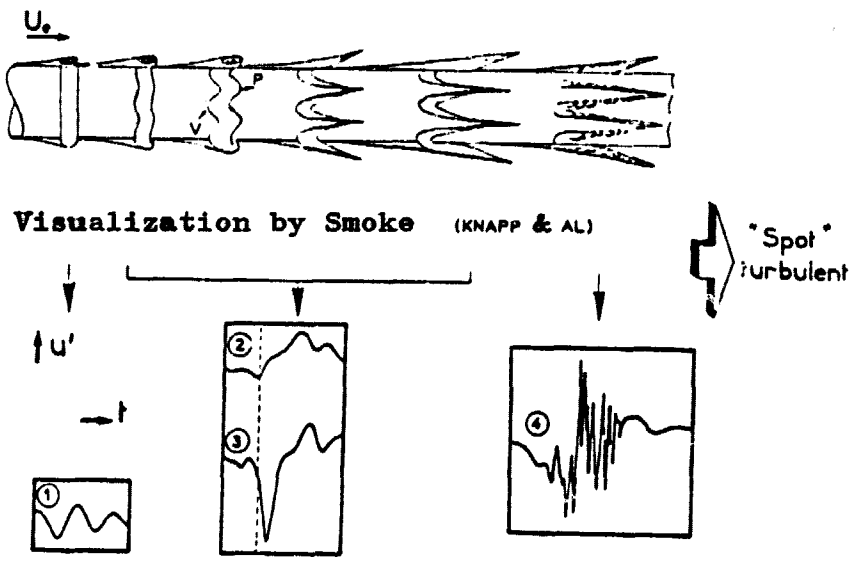

HOT WIRE (Experiments Presented)

Fig. 10 - Appearance of Turbulence
(Configuration A)

Signal ① corresponds to the nondeformed Tollmien-Schlichting waves which have been studied in the preceding paragraph; the

visualizations reveal the passage of these waves in the form of smoke rings surrounding the cylindrical body. After a certain distance, the rings are subjected to a three-dimensional deformation, resulting in a system of "peaks" p and of "valleys" V. This deformation accentuates rapidly: the peaks are subjected to a rising motion in the middle of the boundary layer and are convected to increasingly faster velocities, whereas the valleys remain near the wall, in slow velocity regions. We thus obtain the configuration of a "horseshoe vortex" sloped versus the wall. Signals ② and ③ illustrate this phenonmenon; they are transmitted simultaneously by two hot-wires placed in x = 0.75 m (signal ② and in x = 0.76 m (signal ③), at the same altitude y = 0.45 mm. Between the two stations, it is possible to see the appearance and amplification of a negative fluctuation "points", the amplitude of which measured on signal ③ exceeds 8 m/s, for a mean velocity of 12 m/s. Such a point indicates the passage of a horseshoe vortex, as was demonstrated by the works of Klebanoof-Tidstrom-Sargent (13), of Kyasznay-Komoda-Vasudeva (14) and of Thomson (15). It is important to point out that these points have amplitudes which are ten or twenty times greater than the Tollmien-Schlichting waves and that their appearance is a random occurence.

When the three-dimensional vortex was sufficiently "stretched", i.e. when the negative points have reached a large enough amplitude, the turbulence appears: on the visualizations, the two vortex "arms" seem to burst into smaller structures (breakdown) and lose their identity; signal ④ corresponds to this occurence; it is possible to distinguish a rapid decline in instantaneous velocity (negative point) followed by a sequence of frequency fluctuations considerably larger than those encountered until then: this is the birth of a turbulent "spot".

We may have a better understanding of the passage from the "negative point" stage to the "spot onset" stage by studying the effect of negative points which still have not burst (signal ③) on the instantaneous velocity profile. Accordingly, a calculation

of over-all averages has been performed. If T_p represents the time of a negative point and t the time measured from the beginning of the point, we calculate the average of $u(t)$ (annotated (U_p) over a large number of points, for a given value of t/T_p. By varying t/T_p from 0 to 1, we obtain a sort of model picture of the negative points. Moreover, by working on the signals transmitted simultaneously by two hot-wires placed at different altitudes, we have been able to adjust in time, one versus the other, the over-all averages thus obtained.

Examples of curves $(U_p)(t)$, parametered by the altitude y, are presented on the left part of figure 11. Another representation

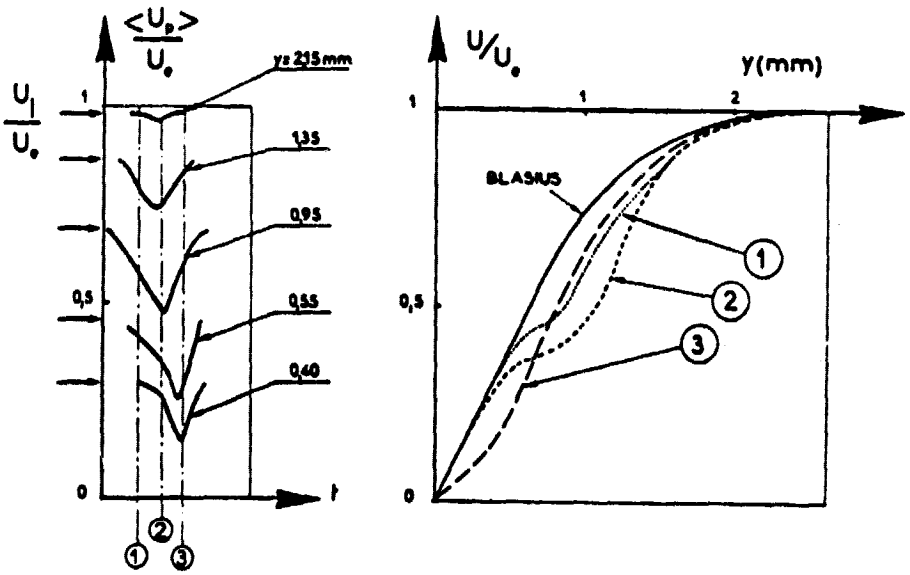

Fig. 11 - Study of the Negative Points of u' (Configuration A, x = 0.75 m)

shown on the right side consists of plotting the instantaneous velocity profiles by considering the values of (U_p) at various instants,

represented by ①, ② & ③. Compared to the Blasius profile, a deformation appears first toward the outside of the boundary layer (profile ①, translating the passage of the "head", or of the "peak", of the horseshoe vortex), and by accentuating (profile ②), it gives an increasingly more distinguishable point of inflexion. Profile ③ shows that the area surrounding the wall is then affected, whereas on the outside, the deformation of profiles ① and ② are reabsorbed (passage from "arms" or from "valleys".

These calculations represent averages over several tens of very different amplitude points. In fact, if we follow one of these points, its amplitude increases very rapidly and the point of inflexion which results on the instantaneous profile becomes so pronounced that the boundary layer becomes unsteady and turbulence /9 appears.

4.2.2. - Case of the Positive Pressure Gradient

Even though the general process is the same for the flat plate, differences appear in the unstabilizing mechanisms of the laminar boundary layer.

We have plotted on figure 12 the variation along y of the factor of dissymmetry $D = \overline{u'^3}/(\overline{u'^2})^{3/2}$ for two abscissas of configuration D; one is selected for the laminar regime (x = 0.40 m), the other is selected for the turbulent regime (x = 0.45). Let us recall that the shape parameter begins to decrease with x = 0.44 m.

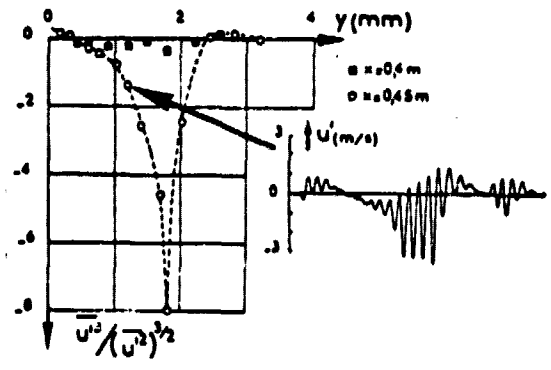

Fig. 12 - Factor of Dissymmetry (Configuration D)

In x = 0.40 m, the factor of dissymmetry keeps very low values in the entire thickness of the boundary layer. In x = 0.45 m, on the other hand, D becomes positive

right next to the wall, then decreases rapidly until it reaches a minimum value of -8, which is reached for y = 1.8 mm, or $y/\delta \simeq 0.5$. Examination of the hot-wire signal makes it possible to understand the origin of these high negative values; an example is given on figure 12, for y = 1.2. It may be observed that the Tollmien-Schlichting waves become deformed and tend to be stretched at lower velocities. This process is similar to that of the appearance of negative points in the case of the flat plate, but with a few differences; the points appear very sporadically, individually or by groups of two and abruptly acquire larger amplitudes with a magnitude at least equal to those of the irregular waves. In the case of the positive pressure gradient, they are rather wave trains with a half dozne elements or more which are "stretched" progressively; no more turbulent fluctuations may be found in the initial phase of the transition (contrary to case A), the decline in H comes only from the deformation of waves.

Knapp-Roache-Mueller visualizations in the case of a transition with positive pressure gradient show that the Tollmien-Schlichting waves undergo a three-dimensional deformation, like in the case of the flat plate, but in the former case, the deformation is more progressive. For example, the horse-shoe vortex peak is very round ("milk-bottle"), whereas it is very pointed in the steady flow.

4.3 - Transition Medium

The expression "transition medium" is in fact rather vague; we are using it here to specify the abscissa where the shape parameter reaches a value of the order of 2, intermediary between the values of transition onset and completion. We shall take into consideration again cases A and D at the stations corresponding respectively to x = 0.94 m (H = 2.1) and x = 0.50 m (H = 2.2).

4.3.1. - Case of the Flat Plate

Figure 13 shows two simultaneous recordings of velocity u(t),

performed near the wall (y = 0.4 mm) and toward the middle of the boundary layer thickness (y = 2.1 mm), together with the corresponding spectra. The hot-wire signals bring about the occurence of intermittence, characterized by the succession of turbulent spots (high frequency fluctuation regions) and of laminar regions, with a rectangular appearance. This figure calls for the following remarks:

Next to the wall, the mean velocity in the turbulent spots is higher than the laminar velocity. When y increases, the effect is the opposite.

The shape of the spots varies from a quasi-rectangular shape near the wall to a highly dissymmetrical, serrated shape at higher altitudes;

No peak or special frequency appear on the spectra.

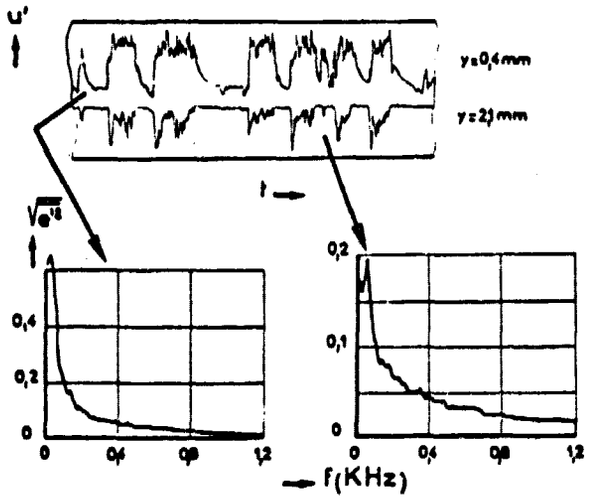

Fig. 13 - Occurence of Intermittence (Configuration A)

We have represented on fig. 14 the diagrammatic shape of a spot in the x-z plane, such that it is possible to deduce visualizations performed by various authors, Elder (16), for example. The front face is convected at a velocity $U_A \simeq 0,9 U_e$ the rear face at a velocity $U_L \simeq 0,5 U_e$ (these values, given for the first time by Schubauer-Klebanoff (17), have been confirmed by our experiments and by those of Cousteix-Houdeville-Desopper (18) in an unsteady flow). The difference in propagation velocity of the front and rear faces explains the development of the spots and their coalenscence progressively into longer, but fewer spots.

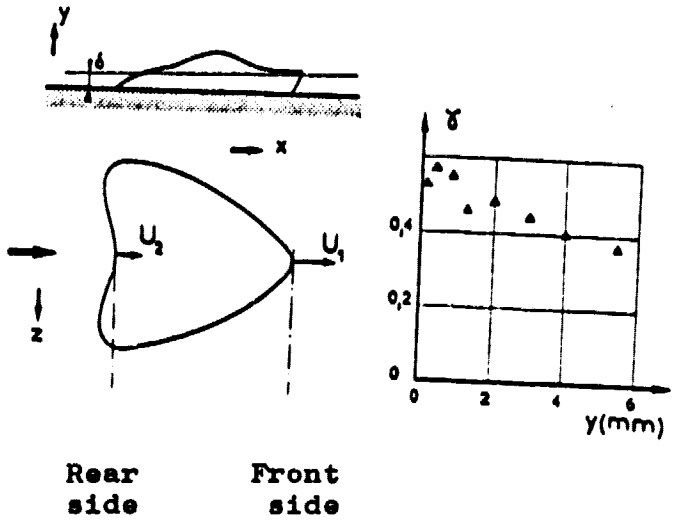

Fig. 14 - Intermittence Factor

The conditional analysis of the effect of intermittence has been the subject of previous publications ((4) and (5)). The detection signal adopted to discriminate the spots of laminar zones is $\left|\frac{\partial u}{\partial t}\right|$, which favors the high frequencies of turbulent structures. Fig. 14 shows the evolution following y of the intermittence factor γ at the station under consideration; γ represents the time ratio where the flow is turbulent during the whole time.

The conditional analysis has shown that the spots, of which the time length exceeded 9 ms, presented a certain number of standard properties of the "established" turbulent boundery layer. Figure 15 shows the over-all averages $\langle u_t \rangle / u_e$ of these spots, calculated at various altitudes. As for the negative points, the curves are set in time one versus the other. It may be observed that these results are comp rable to those obtained by Wygnanski-Sokolov-Friedman (19) and by Cantwell-Coles-Dimotakis (20) in the case of turbulent spots created artificially by electric discharges. It may be observed that the appearance of the spot occurs practically at the same instant in the entire thickness of the boundary layer and

that its time duration (hence the factor of intermittence) diminishes with the altitude starting from its rear face.

On the right side of the figure, four instantaneous profiles

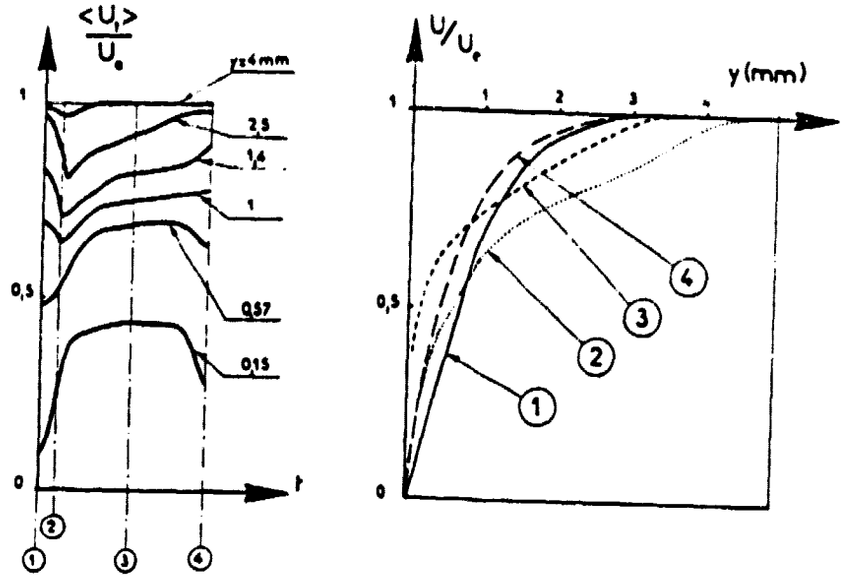

Fig. 15 Study of Turbulence Spots

have been plotted. At the beginning of the spot, the profile , is very similar to a Blasius profile (H congruent to 2.6). Profile shows mainly a considerable increase in instantaneous thickness of the boundary layer and a decrease in the shape parameter; with profile (3), H remains weak (about 1.4 to 1.5), but the thickness of the boundary layer already decreases. At the end of the spot (profile (4), the shape parameter has returned to a value not very different from 2.

4.3.2. - Case of the Positive Pressure Gradient

If we consider now the transitient flow in the positive pressure gradient, significant differences appear versus the case of the

flat plate. These differences are illustrated on figure 16 by two simultaneous recordings performed in configuration D, at the same reduced altitudes y/θ as on figure 13 relative to configuration A. It is not possible to see the appearance here of large individualized structures affecting the traditional shape of the turbulent spots, but rather series of peaks guided toward higher velocities in the proximity of the wall, toward lower velocities at the highest altitudes. The most remarkable characteristic of the corresponding spectra, presented at the bottom of the figure, is the presence of a maximum for a frequency close to 400 Hz, i.e. the frequency of the Tollmien-Schlichting waves studied in the laminar state (§ 4.1.). We have seen at the transition onset (§ 4.2.2.) that these waves are deformed and lengthened; this lengthening has become such that it is found again here on signal u(t) in the form of peaks.

High frequency fluctuations are superposed on some of these peaks, indicating the beginning of the appearance of turbulence; in particular, the recording section marked by hooks is made up of a series of 5 or 6 peaks, keeping their individuality, but on the verge of blending into a single "spot" type structure. This type of signal appearance is in fact rather rare at the abscisse under consideration, and the reduction in the shape parameter from the value 3.1 at the transition onset to the value 2.2 was essentially caused by the increase in amplitude on the peaks, where high frequency fluctuations characteristic of turbulence appear only very rarely.

4.4. - Transition Completion

Considering the preceding observations, we have wanted to see if, at the end of the transition zone (i.e. when H has reached values of about 1,5), there were still any differences in structure between configurations A and D which are as distinct as during the middle of the transition.

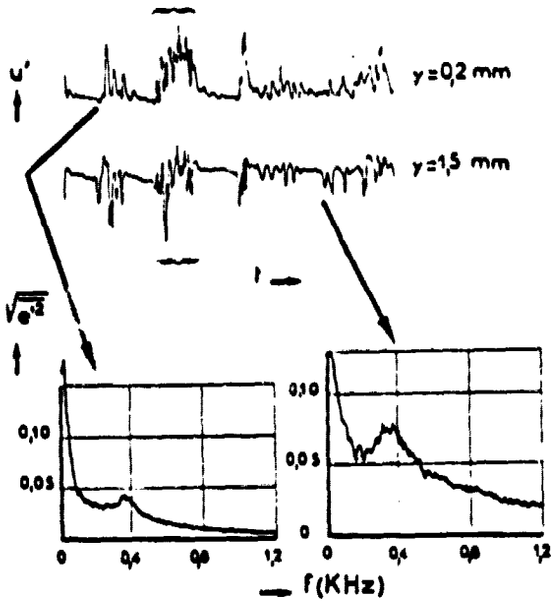

Fig. 16 - Occurance of Intermittence (Configuration D)

Four recordings of the hot-wire signal are presented on figure 17. Two of them occur near the wall for each configuration, the two others occur near the midle of the boundary layer thickness, also for each configuration. /12

It is shown that the two signals recorded in $y/\theta = 0.6$ have very comparable appearances. In case A, the spots have continued to develop; in case D, the peaks have lost their individuality and the signal is composed mainly of high frequency fluctuations; moreover, the spectrum of u' no longer shows a point and spreads substantially at high frequencies.

In $y/\theta = 6$, however, the two signals have less similarity than when near the wall; in the case of the flat plate, the "serrated pattern" already observed in the middle of the transition are found again; in case D, we find again the peaks guided toward lower velocities, but here, they are all "erected" with turbulent fluctuations. It remains to be known what distance is necessary after the end of transition for the two turbulent boundary layers which have undergone transition, one in a decelerated flow, the other in a steady flow, to recover exactly the same structure.

5 - CONCLUSION

The experimental results just presented make it possible to draw a few conclusions relating to the effect of a positive pressure gradient on the location, the length and the transition

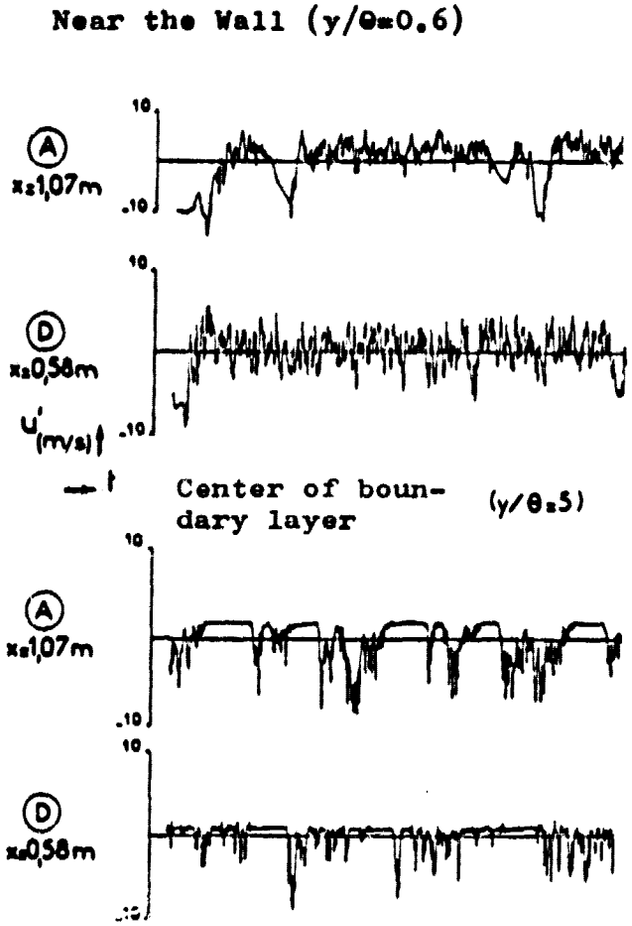

Fig. 17 - Recordings of u' at the end of transition (configuration A and D)

mechanisms of the laminar boundary layer transition in an incompressible flow.

Generally speaking, it seems logical that a deceleration of the external flow considerably diminishes the Reynolds number of transition and the length of transition. By basing the definitions of the points of transition onset and completion on the evolution of the shape parameter, we may assume $\Delta R_\theta \simeq R_{\theta_T}$. In fact, the definition of the transition point is rather difficult, since the turbulence profiles take longer to reach the turbulent state than the mean velocity profiles.

A more thorough study of the processes of turbulence appearance shows that, in all cases, the presence of Tollmien-Schlichting waves as predicting signs of transition. In conformity with the results of the laminar instability theory, these waves are considerably more amplified in the positive pressure gradient than in the flat plate. From the moment where nonlinear occurences enter into play, we find in the case without gradient the rapid amplification of negative fluctuation "points", which unstabilize the laminar boundary layer, thus contributing to the creation of turbulent spots. In the presence of a positive pressure gradient, the Tollmien-Schlichting waves seem "stretched", and the turbulent fluctuations appear individually

on each of them. Only very far within the transition region may the presence of turbulent spots of the type encountered in the steady flow be detected.

REFERENCES

1. Michel R., "Transition and Amplification Criterion of Laminar Instability Waves", La Recherche Aéronautique no. 70 (1959).

2. Dunham J., "Predictions of Boundary Layer Transition on Turbomachinery Blades", Agard Meeting, Boundary Layers in Turbomachines. Paris 1972.

3. Arnal D., Juillen J.C.,"Experimental and Theoretical Investigation of the Boundary Layer Transition", La Recherche Aérospatiale no. 1977-2.

4. Arnal D., Juillen J.C., "The Investigation of Intermittence in a Transition Region", La Recherche Aérospatiale no. 1977-3.

5. Arnal D., Juillen J.C., Michel R., "Experimental Analysis and Calculation of the appearance and Development of the Boundary Layer Transition", AGARD Conference Proc. no. 224. Laminar-Turbulent Transition. Copenhagen, May 2-4, 1977.

6. Klebanoff P.S.,"Characteristics of Turbulence in a Boundary Layer With Zero Pressure Gradient", NACA Report 1-247 (1955).

7. Schubauer G.B., Skramstad H.K., "Laminar Boundary Layer Oscillatins and Transition On A Flat Plate", Report 909, NACA, 1948.

8. Schlichting H.,"Boundary Layer Theory", 6th ed. Mc Graw-Hill, p. 431-522.

9. Jordinson R., "Numerical Integration of the Orr-Sommerfeld Equation", J. Fluid Mech., Vol. 66, Part 3 (1974).

10. Mack L.M.,"Transition Prediction and Linear Stability Theory", AGARD Conference Proc. no. 224. Laminar-Turbulent Transition. Copenhagen, May 2-4, 1977.

11. Obremski H.J., Morkovin M.V., Landahl M., "A Portofolio of Stability Characteristics of Incompressible Boundary Layers", Agardograph no. 134, March 1969.

12. Knapp C.F., Roache P.J., Mueller T.J., "A Combined Visual and Hot-Wire Anemometer Investigation of Boundary Layer Transition", UNDAS-TR-866 CK, August 1966.

13. Klebanoff P.S., Tidstrom K.D., Sargent L.M., "The Three-Dimensional Naure of Boundary Layer Instability", J. Fluid Mech., Vol. 12, Part 1, 1962.

14. Kovasznay L.S.G., Komoda M., Vasudeva B.R., "Detailed Flow Field In Transition", Proc. 1962, Heat Transfer Fluid Mech. Inst. Stanford University Press, 1962, 1-26.

15. Thomson K.D., "The Prediction of Inflexional Velocity Profiles and Breakdown in Boundary Layer Transition", WRE-Report 1052 (WR and D), October 1973.

16. Elder J.W., "An Experimental Investigation of Turbulent Spots and Breakdown to Turbulence", J. Fluid Mech., Vol. 9, Part 2 (1960).

17. Schubauer G.B., Klebanoff P.S., "Contribution on the Mechanics of Boundary Layer Transition", Rept. 1289, 1956, NACA.

18. Cousteix J., Houdeville R., Desopper A., "Transition of a Boundary Layer Subjected To an Oscillation of the External Flow", AGARD Conference Proc. no. 224. Laminar-Turbulent Transition. Copenhagen May 2-4, 1977.

19. Wygnanski I., Sokolov M., Friedman D., "On a Turbulent "Spot" in a Laminar Boundary Layer", J. Fluid Mech., Vol. 78, Part 4, 1976.

20. Cantwell B., Coles D., Dimotakis P., "Structure and Entrainment in the Plane of Symmetry of a Turbulent Spot", J. Fluid Mech., Vol. 87, Part 4, 1978.